

# Precision Motion Control of Hydraulic Actuators with Performance Guaranteed Online Parameter Estimation

Manzhi Qi<sup>b</sup>, Yangxiu Xia<sup>a,b</sup>, Shizhao Zhou<sup>a,b</sup>, Qixian Wang<sup>b</sup>, Deqing Mei<sup>a,b</sup> and Zheng Chen<sup>a,b,\*</sup>

<sup>a</sup>State Key Laboratory of Fluid Power and Mechatronic Systems, Zhejiang University, Hangzhou 310027, China

<sup>b</sup>Ocean College, Zhejiang University, Zhoushan, Zhejiang, 316021, China

**Abstract**—With the development of industrialization, valve-controlled hydraulic actuators are gradually attracting attention for their impressive power-to-weight ratio, high torque/force output, and significant load capacity, and their future application in heavy engineering has great potential. However, due to the complex higher-order nonlinear dynamics as well as the parameter uncertainties and uncertain nonlinearities of hydraulic actuators, the design of their controllers is full of challenges. Moreover, when facing practical work requirements such as load estimation, achieving an ideal position-tracking effect alone may not be sufficient. Accurate parameter estimation becomes equally important in such cases. For this purpose, a direct/indirect adaptive robust controller (DIARC) is proposed in this paper. By incorporating nonlinearities and uncertainties into the dynamic modeling and compensating for them with adaptive robust controllers, the effectiveness of the control can be improved. Furthermore, we have enhanced the traditional adaptive law by integrating not only the tracking error but also the parameter estimation error information. This improvement allows for a more accurate and reliable estimation of the parameter. The control performance is simulated and verified. The simulated results indicate that the implemented controller not only enhances tracking accuracy but also accurately estimates the unknown parameter.

**Index Terms**—adaptive robust control, parameter estimation, valve-controlled hydraulic actuators

## I. INTRODUCTION

The valve-controlled hydraulic actuators, commonly used in hydraulic manipulators, have great application prospects in industrial fields such as oil and gas production, mining industries, civil engineering industries, and other scenarios [1]–[3]. This is attributed to their remarkable power-to-weight ratio, high torque/force output, and substantial load capacity [4]. The existing hydraulic actuators are difficult to meet the increasing requirements of high-precision operation [4], which is because, on the one hand, compared to the motor drive method, the hydraulic actuator has complex higher-order nonlinear dynamics, for example, non-smooth nonlinearities in pressure dynamics, dead zones in valve operation, etc. On the other hand, there are parameter uncertainties and uncertain nonlinearities in the system [5], such as unmodelled friction,

complex flow properties, flow leakages [1], [6], etc, and the system's modeling accuracy can be affected. The control of hydraulic actuators has garnered attention as a significant research area in recent years.

Traditional linear control theories, such as the widely used proportional-integral-derivative (PID) and feedback linearization techniques [7], [8], have found extensive application in hydraulic systems. However, it is important to note that non-model-based linear methods face inherent limitations in achieving high performance when dealing with the inherent complexity and nonlinearities of hydraulic systems. As a result, there is a growing need for advanced control strategies that can effectively address these challenges and enhance the overall performance of hydraulic actuators. Many advanced nonlinear control methods have been developed to improve tracking performance [9], [10]. In [11], Yao and Tomizuka introduced the direct adaptive robust control (DARC) technique for precision motion control in an electro-hydraulic system featuring a single-rod hydraulic actuator. Yao et al. proposed the robust integral of the sign of the error (RISE) controller and combined it with parameter adaptive control to minimize the tracking error of the system. This approach effectively mitigates parameter uncertainties and reduces the tracking error in the hydraulic system [12], [13]. In a separate study, Mattila et al. presented the Virtual Decomposition Control (VDC) approach [14], [15]. This method transforms the control problem of the entire hydraulic system into a subsystem control problem while ensuring system stability. The VDC approach has shown promise in effectively handling various nonlinearities and parameter uncertainties that arise in the system.

While the above methods have displayed excellent results in controlling the accuracy of hydraulic actuators. In certain secondary tasks, such as load estimation [16], the provision of accurate estimates can offer valuable guidance and enhance the precision of dynamic modeling. To achieve this, it is equally imperative to ensure accurate parameter estimation and control effectiveness. In recent decades, there has been extensive research on adaptive parameter estimation [17]. The majority of this research employs gradient descent algorithms, least squares (LS), and projection methods [18], [19]. In the aforementioned controller design, the parameters are estimated

This work is supported by National Natural Science Foundation of China (No.523B1002 and No.52075476), and Natural Science Foundation of Zhejiang Province (No. LR23E050001).

\*Corresponding author. E-mail: zheng\_chen@zju.edu.cn.

utilizing the gradient descent law. This method relies on the position tracking error of the system. However, in practical implementation, the tracking error tends to be exceedingly small. Consequently, the adaptability of the parameters is vulnerable to other overlooked factors, such as sampling delay and noise, thereby impeding optimal parameter convergence speed [20].

Now this paper focuses on one of the arm joints of the hydraulic manipulator, which is driven by a hydraulic actuator. A direct/indirect robust adaptive controller (DIARC) was proposed, and the control law and parameter adaptive law were separated to achieve precise motion control. A new parameter adaptive method is proposed, which obtains parameter estimation error information by introducing filtering variables and auxiliary matrixes. In theory, it ensures the arbitrarily fast exponential convergence of parameters, achieving accurate and fast parameter estimation. Finally, the effectiveness of the algorithm was verified through simulation, and the comparison results showed that the proposed algorithm has precise motion control and accurate parameter estimation effects

## II. PROBLEM FORMULATION

### A. Dynamic Model

In this paper, the valve-controlled hydraulic actuators, generally used in hydraulic manipulator shown in Fig. 1 is considered. In this article, we will utilize the boom joint of the manipulator as our example. The dynamic expression for this joint can be written as follows:

$$I\ddot{q} = J_x(q)F_L - fs(\dot{q}) - B_f\dot{q} + d_1 \quad (1)$$

where  $I$  represents the moment of inertia of the boom joint;  $J_x(q)$  represents the nonsingular joint Jacobian matrix;  $B_f$  and  $f$  represents the viscous friction coefficient and Coulomb friction coefficient;  $s(\bullet)$  represents a smoothing function;  $d_1$  is the modeling error, which includes the nominal value  $d_{1n}$  and deviation amount  $\Delta d_1$ . Same as in [16], the control force of the hydraulic cylinders  $F_L$  can be described as

$$F_L = P_1S_1 - P_2S_2 \quad (2)$$

where  $P_1$  and  $P_2$  are the pressure in the hydraulic cylinder chamber, respectively;  $S_1$  and  $S_2$  are the area of the hydraulic cylinder chamber, respectively. Further, assuming no cylinder leakages, we can obtain the pressure dynamics

$$\begin{aligned} \dot{P}_1 &= \frac{\beta_e}{V_1}(-S_1J_x(q)\dot{q} + Q_1 + d_{21}) \\ \dot{P}_2 &= \frac{\beta_e}{V_2}(S_2J_x(q)\dot{q} - Q_2 - d_{22}) \end{aligned} \quad (3)$$

where  $\beta_e$  is the effective bulk modulus;  $Q_1$  and  $Q_2$  are the supply flow rate of the front chamber and the return flow rate of the return chamber, respectively;  $d_{21}$  and  $d_{22}$  are the nominal values of these uncertainties, which has the same two part  $d_{2in}$  and  $\Delta d_{2in}$  ( $i = 1, 2$ ) as  $d_1$ . The volumes of two different chambers  $V_1$  and  $V_2$  can be further written as

$$\begin{aligned} V_1 &= V_{h1} + S_1x \\ V_2 &= V_{h2} - S_2x \end{aligned} \quad (4)$$

where  $x$  represents the cylinder displacement;  $V_{h1}$  and  $V_{h2}$  are the volumes of the two chambers when  $x$  equals zero. Then, the flow rates  $Q_1$ ,  $Q_2$  and the valve input voltage  $u$  can be mathematically expressed as follows:

$$\begin{aligned} Q_1 &= k_{p1}f_p(P_s - P_1)u\Lambda(u) + k_{v1}f_p(P_1 - P_r)u\Lambda(-u) \\ Q_2 &= -k_{v2}f_p(P_2 - P_r)u\Lambda(u) - k_{p2}f_p(P_s - P_2)u\Lambda(-u) \end{aligned} \quad (5)$$

where  $k_{p1}$ ,  $k_{p2}$ ,  $k_{v1}$ ,  $k_{v2}$  is the conversion coefficient;  $P_s$  is the supply pressure of the fluid;  $P_r$  is the tank of reference pressure, and the  $\Lambda(\bullet)$  is defined as

$$\Lambda(\bullet) = \begin{cases} 1, & \bullet \geq 0 \\ 0, & \bullet < 0 \end{cases} \quad (6)$$

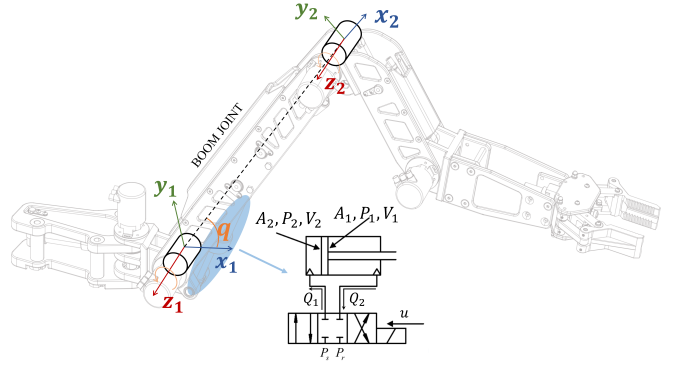


Fig. 1. The diagram of hydraulic manipulator driven by hydraulic actuator

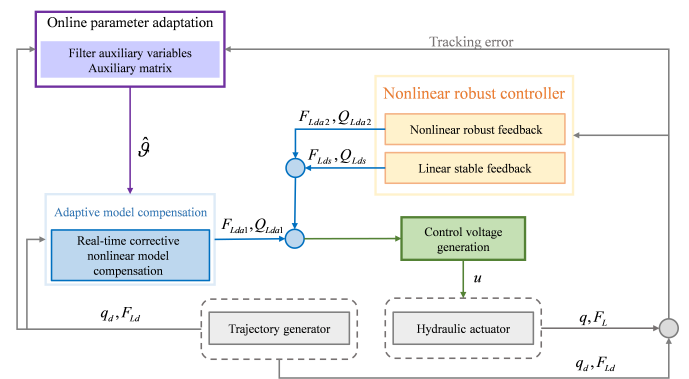


Fig. 2. The algorithm diagram of the controller

and the function  $f_p(\bullet)$  is defined as

$$f_p(\bullet) = \text{sgn}(\bullet)\sqrt{|\bullet|} \quad (7)$$

### B. Parameterization of models

To account for the parametric uncertainties arising from the variations of parameters  $I$ ,  $f$ ,  $B_f$ ,  $d_{1n}$ ,  $\beta_e$ ,  $d_{21n}$  and  $d_{22n}$ , we define the set of unknown parameters as follows:

$$\begin{aligned} \vartheta &= [\vartheta_1, \vartheta_2, \vartheta_3, \vartheta_4, \vartheta_5, \vartheta_6, \vartheta_7]^T \\ &= [I, f, B_f, d_{1n}, \beta_e, d_{21n}, d_{22n}]^T \end{aligned} \quad (8)$$

Although the state space contains  $q, \dot{q}, F_L, P_1, P_2$ , the control variables we need to be concerned with are  $q, \dot{q}, F_L$ . Thus, define  $x = [x_1, x_2, x_3]^T = [q, \dot{q}, F_L]^T$ . The system dynamic (1) and (3) can thus be linearly parameterized in terms of  $\vartheta$  as

$$\dot{x}_1 = x_2 \quad (9)$$

$$\vartheta_1 \dot{x}_2 = J_x(q)F_L - \vartheta_2 s(x_2) - \vartheta_3 x_2 - \vartheta_4 + \Delta d_1 \quad (10)$$

$$\vartheta_5 \dot{x}_3 = -J_x(q)f_1 x_2 + Q_L + f_2 \vartheta_6 + f_3 \vartheta_7 + \Delta d_2. \quad (11)$$

where  $f_1 = (S_1^2/V_1 + S_2^2/V_2)$ ,  $f_2 = (S_1/V_1) d_{1n}$ ,  $f_3 = (A_2/V_2) d_{2n}$ ,  $Q_L = S_1 (Q_1/V_1) + S_2 (Q_2/V_2)$ . For the convenience of understanding and reading in the following section,  $F_L$  will be used instead of  $x_3$ .

**Assumption 1.** The boundary range of parameter uncertainties and uncertainty nonlinearities is known, i.e.,

$$\begin{aligned} \vartheta_{i \min} \leq \vartheta_i \leq \vartheta_{i \max}, i = 1, \dots, 7 \\ |\Delta d_i(t)| \leq \delta d_i(t), i = 1, 2 \end{aligned} \quad (12)$$

where  $\vartheta$  are some unknown constants,  $\vartheta_{i \min}, \vartheta_{i \max}$  and  $\delta d_i(t)$  are known.

### III. CONTROLLER DESIGN AND PARAMETER ESTIMATION

The control block diagram is shown in Fig. 2 To address the high-order dynamics of the hydraulic actuators, a backstepping strategy is employed. The control design has two main objectives: achieving high tracking accuracy and ensuring parameter convergence to their true values.

#### A. control law design

1) *Step 1:* Define a variable  $z_2$  as

$$z_2 = \dot{z}_1 + k_1 z_1 = x_2 - x_r, x_r \triangleq \dot{x}_{1d} - k_1 z_1 \quad (13)$$

where  $z_1 = x_1 - x_{1d}$  represents the tracking error of joint angle,  $k_1$  is the linear feedback gain,  $x_{1d}$  is the desired trajectory. Further, differentiate the  $z_2$ , (9) can be written as

$$\vartheta_1 \dot{z}_2 = J_x(q)F_L - \Psi_1^T \vartheta + \Delta d_1 \quad (14)$$

where  $\Psi_1 = [\dot{x}_r, s(x_2), x_2, 1, 0, 0, 0]^T$ .  $\bullet$  represents the true value,  $\hat{\bullet}$  represents the estimated value, and  $\tilde{\bullet}$  represents the estimated error. Their relationship is written as  $\tilde{\bullet} = \hat{\bullet} - \bullet$ .  $F_L$  is the output thrust of the actual system, and  $F_{Ld}$  is our control thrust, which can be designed as

$$\begin{aligned} F_{Ld} = F_{Lda1} + F_{Lda2} + F_{Lds1} + F_{Lds2} \\ F_{Lda1} = J_x^{-1}(q)\Psi_1^T \hat{\vartheta}, \quad F_{Lds1} = -\vartheta_{1 \min} J_x^{-1}(q)k_{F1} z_2 \end{aligned} \quad (15)$$

where  $F_{Lda1}$  is the feed-forward model compensation.  $F_{Lds1}$  is the linear stable feedback.  $k_{F1}$  is the positive control gain.  $F_{Lda2}$  and  $F_{Lds2}$  are the fast dynamic compensation and robust feedback, respectively, which will be designed in the following part.

Define a variable  $z_3 = F_L - F_{Ld}$ , substituting (13) into (12), we can obtain that

$$\vartheta_1 \dot{z}_2 = -\vartheta_{1 \min} k_{F1} z_2 + \Psi_1^T \tilde{\vartheta} + J_x(q)(F_{Lda2} + F_{Lds2} + z_3) + \Delta d_1 \quad (16)$$

Since  $F_{Ld}$  is not an input that can be directly controlled, we need to further design the virtual flow input  $Q_{Ld}$ .

2) *Step 2:* After designing the desired thrust  $F_{Ld}$  earlier, as  $F_L$  cannot be directly controlled by the input voltage, we further designed to control the flow rate  $Q_L$ , which can be directly controlled by the input voltage. This can be achieved by expressing Eq. (11) as follows:

$$\vartheta_5 \dot{z}_3 = -J_x(q)f_1 x_2 + Q_L - \Psi_2^T \vartheta + \Delta d_2 - \vartheta_5 F_{Ldi} \quad (17)$$

where  $\Psi_2 = [0, 0, 0, 0, \dot{F}_{Ldc}, -f_2, -f_3]^T$ ;  $\dot{F}_{Ldc} = (\partial F_{Ld}/\partial q)\dot{q} + (\partial F_{Ld}/\partial \dot{q})\ddot{q} + (\partial F_{Ld}/\partial t)$  represents the calculable part of  $F_{Ld}$  and  $\dot{F}_{Ldi} = (\partial F_{Ld}/\partial \dot{q})(\ddot{q} - \hat{\ddot{q}}) + (\partial F_{Ld}/\partial \hat{\vartheta})\dot{\hat{\vartheta}}$  represents the incalculable part of  $\dot{F}_{Ld}$ . Thus,  $Q_{Ld}$  can be designed as

$$Q_{Ld} = Q_{Lda1} + Q_{Lda2} + Q_{Lds1} + Q_{Lds2}$$

$$Q_{Lda1} = J_x(q)f_1 x_2 + \Psi_2^T \hat{\vartheta} + Y_Q, \quad Q_{Lds1} = -\vartheta_{5 \min} k_{Q1} z_3 \quad (18)$$

Similar to step 1,  $Q_{Ld}$  and  $F_{Ld}$  have the same structure and function, where  $Y_Q = -J_x(q)(w_1/w_2)$  is designed to balance the order of magnitude,  $w_1$  and  $w_2$  are two dimensionless numbers;  $k_{Q1}$  is the positive control gain. Substituting (18) into (17), it can be rewritten as

$$\begin{aligned} \vartheta_5 \dot{z}_3 = -\vartheta_{5 \min} k_{Q1} z_3 + \Psi_1^T \tilde{\vartheta} + (Q_{Lda2} + Q_{Lds2} + Y_Q) \\ + \Delta d_2 - \vartheta_5 \dot{F}_{Ldi} \end{aligned} \quad (19)$$

Furthermore, modeling uncertainties and parameter uncertainties in Eq. (16) and (19) can be divided into slow changing parts  $d_{ci}$  and fast changing parts  $\Delta_i^*(t)$  ( $i = 1, 2$ )

$$\begin{aligned} d_{c1} + \Delta_1^*(t) &= \Psi_1^T \tilde{\vartheta} + \Delta d_1 \\ d_{c2} + \Delta_2^*(t) &= \Psi_1^T \tilde{\vartheta} + \Delta d_2 - \vartheta_5 \dot{F}_{Ldi} \end{aligned} \quad (20)$$

We define the following projection mapping  $\text{Proj}_{\hat{\vartheta}}(\bullet)$  [21] to maintain parameter estimates within a known bounded range

$$\text{Proj}_{\hat{\vartheta}}(\Delta) = \begin{cases} 0, & \hat{\vartheta}_i = \vartheta_{i \max} \ \& \ \Delta_i > 0 \\ 0, & \hat{\vartheta}_i = \vartheta_{i \min} \ \& \ \Delta_i < 0 \\ \Delta_i, & \text{otherwise} \end{cases} \quad (21)$$

So  $F_{Lda2}$  and  $Q_{Lda2}$  can be designed in the following form

$$\begin{aligned} F_{Lda2} &= -J_x^{-1}(q)\hat{d}_{c1} \\ Q_{Lda2} &= -\hat{d}_{c2} \end{aligned} \quad (22)$$

where  $\hat{d}_{ci}$  represents the estimation of  $d_{ci}$  ( $i = 1, 2$ ), and its update law can be designed in the same way as in [22], which can be written as

$$\dot{\hat{d}}_{ci} = \text{Proj}(\gamma_i z_{i+1}), \quad i = 1, 2 \quad (23)$$

where  $\gamma_i$  represents the constant positive gain. Then, Eq. (16) and (19) can then be written as

$$\begin{aligned} \vartheta_1 \dot{z}_2 &= -\vartheta_{1 \min} k_{F1} z_2 + J_x(q)(F_{Lds2} + z_3) + \tilde{d}_{c1} + \Delta_1^*(t) \\ \vartheta_5 \dot{z}_3 &= -\vartheta_{5 \min} k_{Q1} z_3 + (Q_{Lds2} + Y_Q) + \tilde{d}_{c2} + \Delta_2^*(t) \end{aligned} \quad (24)$$

$F_{Lds2}$  and  $Q_{Lds2}$  should satisfy the condition

$$\begin{aligned} z_2 F_{Lds2} &\leq 0 \\ z_3 Q_{Lds2} &\leq 0 \end{aligned} \quad (25)$$

and

$$\begin{aligned} z_2 \left( J_x(q) F_{Lds2} + \tilde{d}_{c1} + \Delta_1^*(t) \right) &\leq \xi_1 \\ z_3 \left( Q_{Lds2} + \tilde{d}_{c2} + \Delta_2^*(t) \right) &\leq \xi_2 \end{aligned} \quad (26)$$

where  $\xi_1$  and  $\xi_2$  is an arbitrarily small constant. There are many  $F_{Lds2}$  and  $Q_{Lds2}$  that can meet the conditions, one possible form is

$$\begin{aligned} F_{Lds2} &= -k_{F2} z_2, k_{F2} = \frac{1}{4\xi_1} (d_{c1M} + \|\Psi_1\| \|\vartheta_M\|)^2 \\ Q_{Lds2} &= -k_{Q2} z_3, k_{Q2} = \frac{1}{4\xi_2} (d_{c2M} + \|\Psi_2\| \|\vartheta_M\|)^2 \end{aligned} \quad (27)$$

where  $\vartheta_M = |\vartheta_{max} - \vartheta_{min}|$  and  $d_{ciM}$  represents the upper bound of  $d_{ci}$ , ( $i = 1, 2$ ). We design the first Lyapunov function as  $V_o = (1/2) w_1 \vartheta_1 z_2^2 + (1/2) w_2 \vartheta_5 z_3^2$ . Combining with the condition (25) (26) and Eq.(24), the  $V_o$  can be obtained as follows:

$$\begin{aligned} \dot{V}_o &= w_1 \vartheta_1 z_2 \dot{z}_2 + w_2 \vartheta_5 z_3 \dot{z}_3 \\ &\leq -w_1 \vartheta_{1min} k_{F1} z_2^2 - w_2 \vartheta_{5min} k_{Q1} z_3^2 + \xi_1 + \xi_2 \\ &\leq -\lambda_1 V_o + \nu \end{aligned} \quad (28)$$

with  $\nu = \xi_1 + \xi_2$ .

### B. Parameter estimation

In this section, stable filtering variables and auxiliary matrixes are introduced to design a new parameter adaptive law. Firstly, in order to simplify the problem, we will not consider uncertainty  $\Delta d_i$  and regard it as 0, since  $\Delta d_i$  is bounded. Eq. (10) and (11) can be rewritten as

$$\begin{aligned} \tau_1 &= J_x(q) F_L = \phi_1^T \vartheta \\ \tau_2 &= Q_L - J_x(q) f_1 x_2 = \phi_2^T \vartheta \end{aligned} \quad (29)$$

where

$$\begin{aligned} \phi_1 &= [\dot{x}_2, s(x_2), x_2, 1, 0, 0, 0]^T \\ \phi_2 &= [0, 0, 0, 0, \dot{x}_3, -f_2, -f_3]^T \end{aligned} \quad (30)$$

First, we define an auxiliary variable  $\Omega$  as

$$\dot{\Omega}_i = -l\Omega_i + \tau_i \quad (i = 1, 2) \quad (31)$$

where  $l > 0$  is a constant selected by designed. To simplify the process of parameter estimation, we introduce auxiliary variables defined as follows:

$$\begin{cases} k\dot{\Omega}_{if} + \Omega_{if} = \Omega_i, & \Omega_{if}(0) = 0 \\ k\dot{\tau}_{if} + \tau_{if} = \tau_i, & \tau_{if}(0) = 0 \\ k\dot{\phi}_{if} + \phi_{if} = \phi_i, & \phi_{if}(0) = 0 \end{cases} \quad (32)$$

where  $k > 0$  is the constant;  $\tau_{if}$  and  $\phi_{if}$  are filtered variable with respect to  $\tau_i$  and  $\phi_i$ , ( $i = 1, 2$ ).

Next, define two auxiliary matrix  $P_1, P_2 \in \mathbb{R}^{7 \times 7}$  and  $Q_1, Q_2 \in \mathbb{R}^{7 \times 1}$ , which satisfy the following relationship

$$\begin{cases} \dot{P}_i = -lP_i + \phi_{if} \phi_{if}^T, & P_i(0) = 0 \\ \dot{Q}_i = -lQ_i + \phi_{if} \left( \frac{\Omega - \Omega_f}{k} + l\Omega_f \right), & Q_i(0) = 0 \end{cases} \quad (33)$$

where  $l > 0$  is the same as (31). It is not difficult to find that  $Q_i = P_i \vartheta$ . Then, denote a vector  $W_i$

$$W_i = P_i \hat{\vartheta} - Q_i \quad (i = 1, 2) \quad (34)$$

Based on (34), we can design the parameter adaptive law as:

$$\dot{\hat{\vartheta}} = -\Gamma_1 W_1 - \Gamma_2 W_2 \quad (35)$$

with  $\Gamma_1, \Gamma_2 \in \mathbb{R}^{7 \times 7}$  being an adaptive update gain According to [23], if  $\phi_i$  satisfies the persistently excited (PE) condition, then the auxiliary matrix  $P_i$  is positively definite, i.e.  $\lambda_{min}(P_i) > \mu_i > 0$  for positive constant  $\mu_i > 0$ , ( $i = 1, 2$ ).

We design the second Lyapunov function as  $V_s = V_o + (1/2) \tilde{\vartheta}^T \Gamma_1^{-1} \tilde{\vartheta} + (1/2) \tilde{\vartheta}^T \Gamma_2^{-1} \tilde{\vartheta}$ , the derivation of  $V_s$  is

$$\begin{aligned} \dot{V}_s &= \dot{V}_o - \tilde{\vartheta}^T \Gamma_1^{-1} \dot{\tilde{\vartheta}} - \tilde{\vartheta}^T \Gamma_2^{-1} \dot{\tilde{\vartheta}} \\ &= \dot{V}_o + \tilde{\vartheta}^T P_1 \tilde{\vartheta} + \tilde{\vartheta}^T P_2 \tilde{\vartheta} \\ &\leq -\lambda_2 V_s + \nu \end{aligned} \quad (36)$$

**Theorem 1.** By solving the equation(36), we can obtain the non-negative function  $V_s$  has the following expression

$$V_s(t) \leq \exp(-\lambda_2 t) V_s(0) + \frac{\nu}{\lambda_2} [1 - \exp(-\lambda_2 t)] \quad (37)$$

with  $\lambda_2 = \min \left\{ \frac{2\vartheta_{1min} k_{F1}}{\vartheta_{1max}}, \frac{2\vartheta_{5min} k_{Q1}}{\vartheta_{5max}}, \frac{2\mu_1}{\lambda_{max}(\Gamma_1^{-1})}, \frac{2\mu_2}{\lambda_{max}(\Gamma_2^{-1})} \right\}$  and  $\nu = \xi_1 + \xi_2$ .

**Theorem 2.** If the continuous incentive conditions are satisfied,  $\hat{\vartheta}$  will only converge to its true value when the parameters are uncertain. According to Theorem 1, zero angular tracking error can be achieved, i.e. as  $z_1 \rightarrow 0$  when  $t \rightarrow \infty$ .

## IV. SIMULATION RESULT

### A. Simulation Setup

In order to confirm the efficacy of the controller and parameter estimation method proposed in this paper, we will compare it with the DARC controller mentioned in [24] during the simulation. However, as the controller in [24] is designed for a multi-degree-of-freedom hydraulic manipulator, we simplified the comparison by focusing only on the boom joint.

The simulation parameters for the proposed controller in this paper are set to:  $k_1 = 40, k_{F1} = 40, k_{Q1} = 80$ .  $k_{F2}$  and  $k_{Q2}$  are not involved because condition (25) and (26) can be satisfied when  $k_{F1}$  and  $k_{Q1}$  is sufficiently large. The initial value of  $\hat{d}_{ci}$  is set to:  $\hat{d}_{c1}(0) = \hat{d}_{c2}(0) = 0$ . The adaptive gain of  $\hat{d}_{ci}$  is  $\gamma_1 = 8e^{-5}, \gamma_2 = 6e^{-7}$ . The parameter adaptive rates are set to:  $\Gamma_1 = \text{diag}([15, 10, 10, 10]), \Gamma_2 = \text{diag}([1e^{-6}, 2e^{-2}, 2e^{-2}])$ . The maximum and minimum values of parameter estimates are:  $\vartheta_{max} = [20, 10, 10, 1e^5, 1e^{-8}, 1e^2, 1e^2]^T$ ,

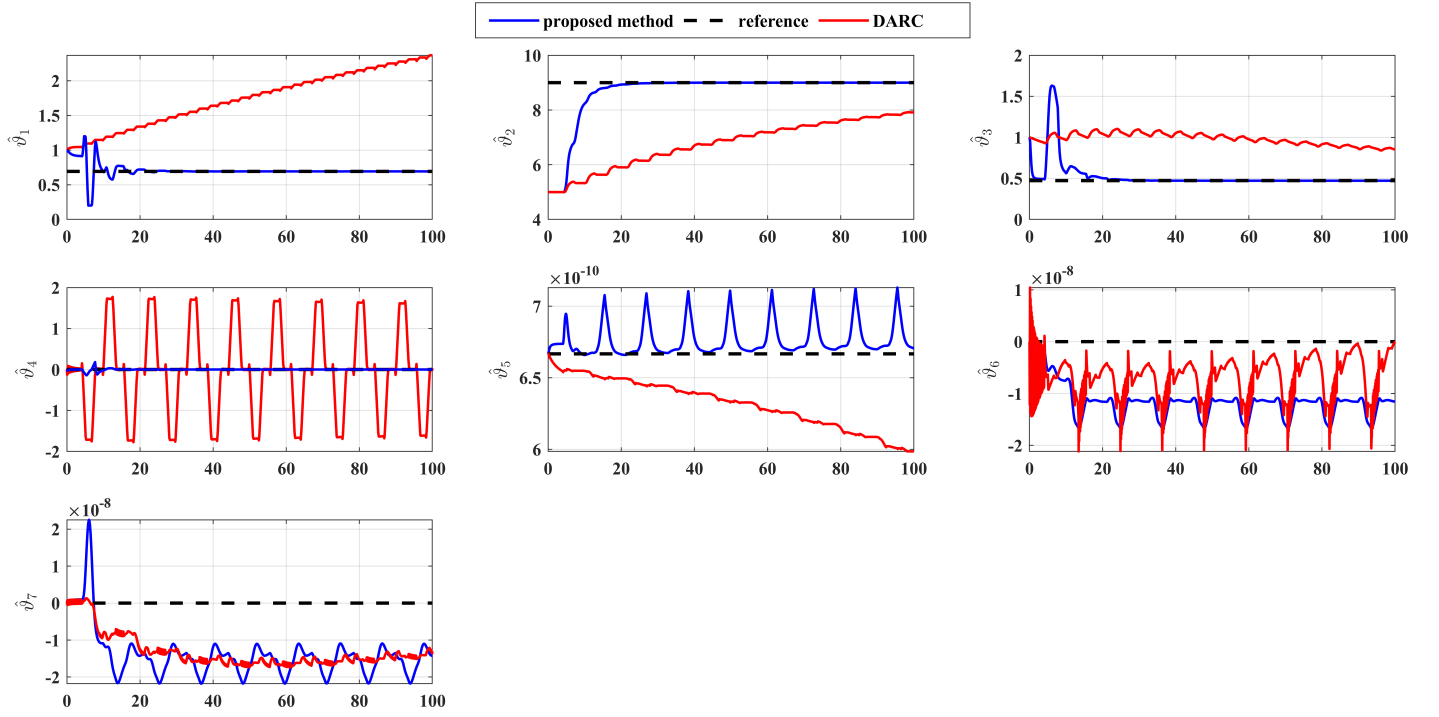


Fig. 3. Adaptive curves for each unknown parameter

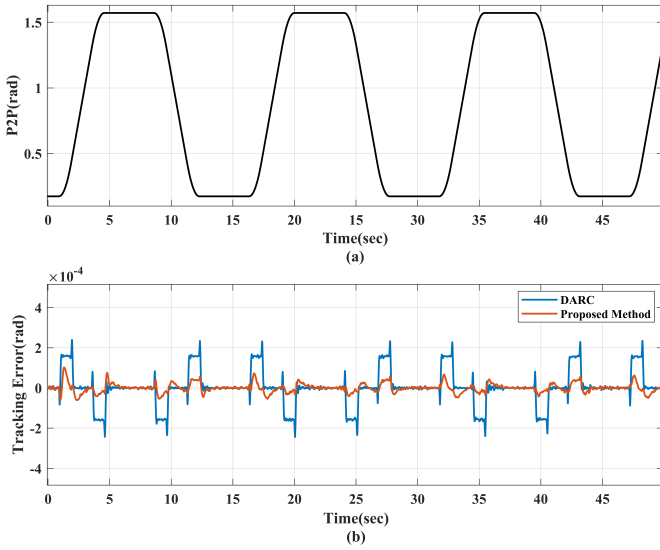


Fig. 4. (a) Desired point-to-point trajectory (P2P). (b) Comparison of tracking errors between different controllers

$\vartheta_{min} = [0.2, 1, 0.1, -1e^5, 5e^{-10}, -1e^2, -1e^2]^T$ . The initial value of parameter estimation is set to:  $\hat{\vartheta}(0) = [1, 5, 1, 0, 1/(1.5e^9), 0, 0]^T$ . The filter coefficient  $k = 0.006$  and the constant  $l = 1$ . To ensure the credibility of the simulation, we ensured that the parameters of the DARC and the controller designed in this paper remained consistent.

We used point-to-point trajectory (P2P) as the expected trajectory. Fig. 4 shows the curves of P2P trajectory and tracking error. The P2P trajectory has three stages: stationary, constant velocity and constant acceleration, which can effectively verify the controller's performance in different motion states. In addition, the P2P trajectory is still third-order differentiable, which meets the requirements of trajectory control during the design process. The upper and lower limits of the P2P trajectory range from 0.17 to 1.57 rad, which is consistent with the angle activity range in actual operations.

### B. Comparative Results

The tracking errors of both controllers are depicted in Figure 4(b). A noticeable improvement in control error is observed with the proposed controller as compared to DARC. The maximum error achieved by DARC is  $2.3 \times 10^{-4}$  rad, whereas the error obtained using the proposed method is  $7.11 \times 10^{-5}$  rad. At approximately 8.5 seconds of sudden acceleration changes, it is notable that DARC produces substantial errors because of its limited ability to promptly adjust to changes in acceleration. Nevertheless, this article's employment of the DIARC allows for fast compensation regarding quick changes in motion through the inclusion of the fast dynamic compensation terms  $F_{Lda2}$  and  $Q_{Lda2}$ , resulting in improved control performance. In addition, in terms of control performance, especially when tracking uniform acceleration, there is a steady-state error in DARC. This is because the control gain of DARC is insufficient (in order to make the results convincing, the

control gains of the two controllers are the same), which leads to a decrease in its tracking effect. On the contrary, this article's proposed controller manifests commendable control efficacy against static, uniform speed, and uniform acceleration motion effects.

The Fig. 3 shows the parameter estimation results of different methods. We can find that compared to DARC, the method proposed in this paper is very accurate for parameter estimation. The physical meaning of  $\vartheta_4$ ,  $\vartheta_6$ , and  $\vartheta_7$  is modeling error and uncertain nonlinearities, which is zero in the case of accurate modeling. However, in Fig. 3, although these three values fluctuate, they persist around zero, and the magnitude of  $\vartheta_6$  and  $\vartheta_7$  is only approximately  $10^{-8}$ , which could be regarded as equivalent to zero. Although  $\vartheta_6$  and  $\vartheta_7$  in the figure have larger fluctuations than DARC, due to their uncertainty in physical meaning, we only focus on their powers. Because in accurately modeled practical systems, its value is theoretically zero. The parameters can converge to the true value in about 15 seconds, and accurate parameter estimation can make the controller's model feed-forward compensation more accurate, thereby achieving the effect of improving control accuracy.

## V. CONCLUSION

This paper presents the design of a direct/indirect adaptive robust controller (DIARC) tailored for the precision motion control of a hydraulic actuator. The DIARC architecture effectively decouples the control law from the parameter adaptive law, mitigating the vulnerability of the parameter adaptive process to external interferences, such as sampling delays and noise, particularly in scenarios where the tracking error is minimal. By introducing auxiliary filtering variables and auxiliary matrices, a new parameter adaptive law is formulated to facilitate precise estimation of unknown parameters, thereby enhancing the effectiveness of motion control. Comparative simulation results demonstrate that, in comparison to the conventional DARC, the proposed DIARC exhibits superior parameter estimation and tracking accuracy under identical control and parameter adaptive gains.

## REFERENCES

- [1] L. Lyu, Z. Chen, and B. Yao, "Advanced valves and pump coordinated hydraulic control design to simultaneously achieve high accuracy and high efficiency," *IEEE Transactions on Control Systems Technology*, vol. 29, no. 1, pp. 236–248, 2021.
- [2] L. Fang, T. Wang, W. Zheng, Z. Liu, L. Ming, X. Zheng, and M. Wu, "Consistency optimal coordination control of underground heavy-load robot in nonstructural environment," *Robotics and Autonomous Systems*, vol. 159, p. 104281, 2023.
- [3] R. Capocci, G. Dooley, E. Omerdić, J. Coleman, T. Newe, and D. Toal, "Inspection-class remotely operated vehicles—a review," *Journal of Marine Science and Engineering*, vol. 5, no. 1, p. 13, Mar. 2017.
- [4] Mattila, Jouni and Koivumäki, Janne and Caldwell, Darwin G. and Semini, Claudio, "A survey on control of hydraulic robotic manipulators with projection to future trends," *IEEE/ASME Transactions on Mechatronics*, vol. 22, no. 2, pp. 669–680, 2017.
- [5] W. Chang, Y. Li, and S. Tong, "Adaptive fuzzy backstepping tracking control for flexible robotic manipulator," *IEEE/CAA Journal of Automatica Sinica*, vol. PP, pp. 1–9, 02 2018.
- [6] Y. Yang, J. Tan, and D. Yue, "Prescribed performance control of one-dof link manipulator with uncertainties and input saturation constraint," *IEEE/CAA Journal of Automatica Sinica*, vol. 6, pp. 148–157, 2019.
- [7] H. Angue Mintsu, R. Venugopal, J.-P. Kenne, and C. Belleau, "Feedback linearization-based position control of an electrohydraulic servo system with supply pressure uncertainty," *IEEE Transactions on Control Systems Technology*, vol. 20, no. 4, pp. 1092–1099, 2012.
- [8] G. Vossoughi and M. Donath, "Dynamic Feedback Linearization for Electrohydraulically Actuated Control Systems," *Journal of Dynamic Systems, Measurement, and Control*, vol. 117, no. 4, pp. 468–477, 12 1995.
- [9] J. Yao, W. Deng, and Z. Jiao, "Adaptive control of hydraulic actuators with lugre model-based friction compensation," *IEEE Transactions on Industrial Electronics*, vol. 62, no. 10, pp. 6469–6477, 2015.
- [10] B. Yao, M. Al-Majed, and M. Tomizuka, "High-performance robust motion control of machine tools: an adaptive robust control approach and comparative experiments," *IEEE/ASME Transactions on Mechatronics*, vol. 2, no. 2, pp. 63–76, 1997.
- [11] B. Yao, F. Bu, J. Reedy, and G.-C. Chiu, "Adaptive robust motion control of single-rod hydraulic actuators: theory and experiments," *IEEE/ASME Transactions on Mechatronics*, vol. 5, no. 1, pp. 79–91, 2000.
- [12] J. Yao, W. Deng, and Z. Jiao, "Rise-based adaptive control of hydraulic systems with asymptotic tracking," *IEEE Transactions on Automation Science and Engineering*, vol. 14, no. 3, pp. 1524–1531, 2017.
- [13] Z. Yao, J. Yao, and W. Sun, "Adaptive rise control of hydraulic systems with multilayer neural-networks," *IEEE Transactions on Industrial Electronics*, vol. 66, no. 11, pp. 8638–8647, 2019.
- [14] J. Koivumäki and J. Mattila, "The automation of multi degree of freedom hydraulic crane by using virtual decomposition control," in *2013 IEEE/ASME International Conference on Advanced Intelligent Mechatronics*, 2013, pp. 912–919.
- [15] J. Koivumäki and J. Mattila, "Stability-guaranteed force-sensorless contact force/motion control of heavy-duty hydraulic manipulators," *IEEE Transactions on Robotics*, vol. 31, no. 4, pp. 918–935, 2015.
- [16] A. Mohanty and B. Yao, "Indirect adaptive robust control of hydraulic manipulators with accurate parameter estimates," *IEEE Transactions on Control Systems Technology*, vol. 19, no. 3, pp. 567–575, 2011.
- [17] S. G. Anavatti, F. Santoso, and M. A. Garratt, "Progress in adaptive control systems: past, present, and future," in *2015 International Conference on Advanced Mechatronics, Intelligent Manufacture, and Industrial Automation (ICAMIMIA)*, 2015, pp. 1–8.
- [18] K. I. Krstic M., Kokotovic P. V., "Nonlinear and adaptive control design," *Wiley-Interscience New York*, vol. 5, no. 2, pp. 4475–4480, 1995.
- [19] E. Abd-Elrady and J. Schoukens, "Least squares periodic signal modeling using orbits of nonlinear odes and fully automated spectral analysis," *IFAC Proceedings Volumes*, vol. 37, no. 13, pp. 345–350, 2004.
- [20] J. Na, X. Ren, and Y. Xia, "Adaptive parameter identification of linear siso systems with unknown time-delay," *Systems & Control Letters*, vol. 66, pp. 43–50, 2014.
- [21] X. Liu, Z. Chen, Y. Liu, F. Duan, C. Yang, and B. Yao, "Direct optimization based compensation adaptive robust control of nonlinear systems with state and input constraints," *IEEE Transactions on Industrial Informatics*, vol. 17, no. 8, pp. 5441–5449, 2021.
- [22] B. Yao, "Adaptive robust control: theory and applications lap integrated design of intelligent and precision mechatronic systems," in *2004 International Conference on Intelligent Mechatronics and Automation, 2004. Proceedings.*, 2004, pp. 35–40.
- [23] J. Na, M. N. Mahyuddin, G. Herrmann, X. Ren, and P. Barber, "Robust adaptive finite-time parameter estimation and control for robotic systems," *International Journal of Robust and Nonlinear Control*, vol. 25, no. 16, pp. 3045–3071, Nov. 2015.
- [24] S. Zhou, C. Shen, Y. Xia, Z. Chen, and S. Zhu, "Adaptive robust control design for underwater multi-dof hydraulic manipulator," *Ocean Engineering*, vol. 248, p. 110822, 2022.